*International Journal of Engineering Science Invention*

*Volume 2 Issue 2 ‖ February. 2013*

# Surface Error Compensation in HSM of Thin Wall Structures

Pal Pandian P[1], Dr.Prabhu Raja V[2], Sakthimurugan K[3]

[1] *Research Scholar, Anna University of Technology, Coimbatore, Tamilnadu, India*
[2] *Associate Professor, Department of Mechanical Engineering, PSG College of Technology, Coimbatore, India*
[3] *Assistant Professor, Department of Mechanical Engineering, M.P.N.M.J Engineering College,Erode*

**ABSTRACT :** *Machining of thin-walled parts is a keyprocess in aerospaceindustry. Many components used in the aerospaceindustry are usually thin-walled structures. Because of theirpoorstiffness, thin-walledworkpieces are veryeasy to deformunder the action of cutting force in the process of cutting. Even in CNC milling, in which the tools are controlledexactlyaccording to the contour of the thin-walled component, the wallwillbethickerat the top and thinnerat the root. In general, the surface errorisinducedmainly by the deflection of the workpieceduringmilling, whichdoes not remove the material as planned. The part deflectioncaused by the cutting force isdifficult to predict and control. The main objective of thisworkis to compensate the surface errorwhichisinduced in machining of thin-walled components. This workinvolvesthree modules such as cutting force modeling, part deformationmodeling and error compensation modeling. A predictivecutting force model has been developed and influence of cuttingparameters on force components and chip thickness has been depicted as graphs usingmathematicaltoolMathCAD 8 professional.*

*The values of force components are validated by experimentsusing 8 channelkistlerdynamometers and on-line/off loneerrormeasurementwillbecarried out using CMM/displacementsensors. Using the force model as input the deformation model has been developed in ANSYS 12.0 and influences unit linearload, cutter location and part thickness on deformation have been plotted as graphs. Finally, the error compensation profile willbedrawn and simulatedusing an NC simulation tool VERICUT 6.0 experimental validation willalsobedone in order to compare the accuracy in dimensions of the component before and aftererror compensation. In future, a commonerror compensation strategycanbedeveloped to integratewith the CNC simulation tools and adopted to industries.*

**Keywords -***High Speed Machining[HSM], Thin walled parts or Thin ribs, surface error, error compensation.*

## I. INTRODUCTION

In the aviation industry, the thin-walled structural parts are widely used. Machining of thin-walled parts is a key process in aerospace industry. Many components used in the aerospace industry are usually thin-walled structures. Because of their poor stiffness, thin-walled work pieces are very easy to deform under the action of cutting force in the process of cutting. Even in CNC milling, in which the tools are controlled exactly according to the contour of the thin-walled component, the wall will be thicker at the top and thinner at the root. In general, the surface error is induced mainly by the deflection of the work piece during milling, which does not remove the material as planned [1,2].

As for the problem of controlling the precision of thickness in the machining of thin-walled components, Russia has applied a cone miller which has special angles to machine thin-walled components, but it cannot solve the problem thoroughly. There are some limitations to this method. High speed machining is a new approach to solve the problem, but it needs a high speed-milling machine[1]. Hence high speed machining technique has been adopted for machining thin ribs. The newer materials such as composite materials, heat resistant and stainless steel alloys, bimetals, compact graphite iron, hardened tool steels, aluminum alloys etc., needs this new machining (HSM)[11].

Machining of materials at four to six times the cutting speed used in conventional machining is called as High Speed Machining (HSM)[11]. HSM is one of the modern technologies, which in comparison with conventional cutting enable to increase the efficiency; accuracy and quality of the work piece and at the same time decrease the cost and machining time. The HSM technology allows the manufacturing of products with excellent surface finish with relatively little increase in total machining time.

Carl Salomon conceived the concept of HSM after conducting a series of experiments in 1924-31. His research showed that the cutting temperature reached a peak value when the cutting speed is increased and the temperature decreases for a further increase of cutting speed. The increase in cutting speed demands a new type of machining system like the machine tool, cutting tool, CNC program etc. The use of high feed rate with high

speed increases the metal removal rate, but the machine in turn requires lighter inertia tables, powerful motor drives and more responsive control systems[12]. One definition of HSM states that, it is an end milling operation at high rotational speeds and high surface feeds. HSM normally uses a high speed in excess of 1000 m/min, feed rates above 1m/min and spindle speeds greater than 10,000 rpm.
This paper presents a predictive force modeling and simulation by MathCAD 8 professional. The force model is then validated by experiments using dynamometers. The deformation analysis is also carried out using ANSYS 12.0 and error compensation strategy is developed[5].

## II. PROBLEM DEFINITION

The machining sketch of the typical thin-walled work piece (Fig. 1) illustrates the deformation of the thin-walled structure in the machining process.

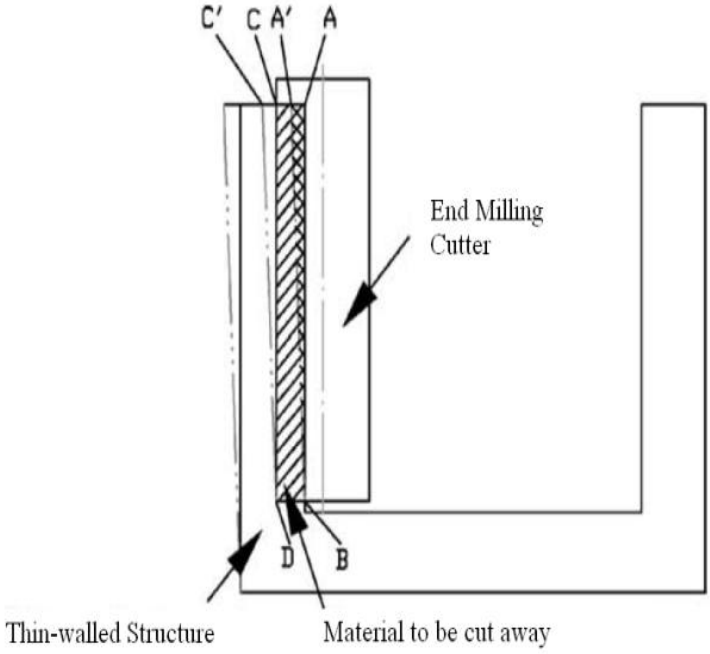


**Fig. 1.Machining sketch of the typical thin-walled structure.**

The material ABDC needs to be cut away ideally. However, under the acting of milling force, Point C moves to Point C' and the Point A moves to Point A'. Therefore, only material A'BDC is cut away in the practical machining process due to the deformation. After the miller moves away from the milling surface, the wall recovers elastically, and material CDC' that should have been cut away remains unremoved. This causes the shape of the wall to be thicker in its higher part and thinner in its lower part. This is the most common problem in the machining of thin-walled components[1,3].

## III. MODELLING OF CUTTING FORCES USING PREDICTIVE MACHINING THEORY

### 3.1 The Predictive Machining Theory

A new approach for modeling and simulation of the cutting forces in helical end milling processes is presented (Fig. 2). In this approach, the cutting forces in helical end milling are modeled based on a predictive machining theory, in which the machining characteristic factors are predicted from input data of fundamental work piece material properties, tool geometry and cutting conditions.

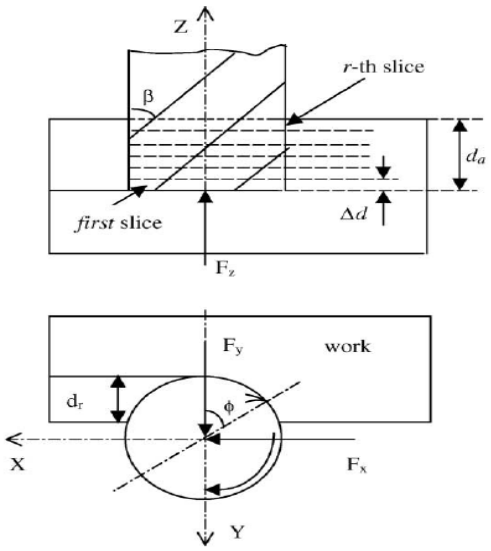


**Fig. 2.Model for End milling Process**

In the model, each tooth of a helical end milling cutter is discretised into a number of slices along the cutter axis to account for the helix angle effect on the cutting forces[13]. The cutting action of each of the slices is modeled as an oblique cutting process. The total cutting forces acting on the cutter is obtained as the sum of the forces at all the cutting slices of all the teeth.

When the tool rotates without any vibration, each axial cutting edge segment, which has a length of $\Delta d=d_a/r$, removes a sinusoidally varying chip thickness. If the feed per tooth is denoted as ft , then this varying undeformed chip thickness can be expressed as,

$$h_{u,v} = f_t \sin\phi_{u,v}, \qquad (1)$$

where$\varphi_{u,v}$ is the angular position of the cutting point of the *u*th flute in the *v*th cutting element (i.e., the *v*th slice), with respect to the negative y direction and measured clockwise. The index of the cutting flutes $u = 1,2,....N_t$ , where $N_t$ is the number of teeth (or flutes) of the tool, and for a right-hand end mill cutter, the flute entering sequence is $1,2,....,N_t$. The index of the cutting slices $v = 1,2,....,r$, where *r* is the number of slices in the axial direction, and the first slice is located in the cutting ends, as shown in Fig. 2. From the geometrical relationship, $\varphi_{u,v}$is given by,

$$\phi_{u,v}(t) = 2\pi nt - (u-1)\frac{2\pi}{z} - (v-1)\frac{2d_a \tan\beta}{rD} \qquad (2)$$

where*n* is the rotating speed of the tool, *t* is the time, *D* is the cutter diameter.

### 3.2 Force Model for Oblique Cutting

In predictive machining theory for an oblique cutting process, the forces acting in cutting, feed and radial directions $P_1$, $P_2$ and $P_3$, respectively as shown in Fig. 3.

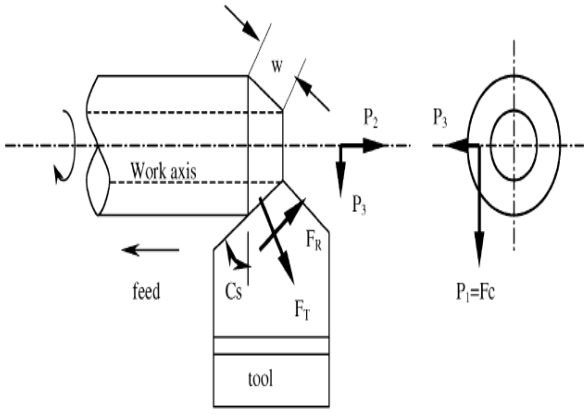


**Fig. 3.Model for simple oblique cutting.**

These forces can be calculated using Eq. (3)

$$P_1 = F_C,$$
$$P_2 = F_T \cos C_S, \quad (3)$$
$$P_3 = F_T \sin C_S - F_R \cos C_S,$$

Where $C_S$ is the tool side cutting edge angle, FC, FT and FR are the force components in the cutting, feed and radial directions, respectively, when CS = 0 and can be calculated using Eqs. (4)-(6).

$$F_C = R\cos(\lambda - \alpha_n), \quad (4)$$
$$F_T = R\sin(\lambda - \alpha_n), \quad (5)$$
$$F_R = \frac{F_C(\sin i - \cos i \sin\alpha_n \tan\eta_c) - F_T \cos\alpha_n \tan\eta_c}{\sin i \sin\alpha_n \tan\eta_c + \cos i} \quad (6)$$

Where $\lambda$ is the mean angle of friction at the tool chip interface, $\alpha_n$ is the tool normal rake angle, $\eta_c$ is the chip flow angle and R is the resultant force at the shear plane and tool–chip interface, and is calculated using the equation,

$$R = \frac{k_{AB} t_1 w}{\sin\phi\cos\theta} \quad (7)$$

Where $k_{AB}$ is the shear flow stress along the shear plane, $t_1$ is the undeformed chip thickness, w is the width of cut, $\varphi$ is the shear angle and $\theta$ is the angle made by R with the shear plane.

### 3.3 Modeling of end milling forces

A milling process can be modeled as the simultaneous processes of cutting with a number of single-point cutting tools (tools having only one major cutting edge)[2,13]. By discretizing the cutting part of a helical end milling tool into r number of slices along its axis in the z direction to account for the helix angle $\beta$, and modeling the cutting action of an individual tooth within each slice as single point oblique cutting which has an inclination angle of $\beta$, cutting edge exist, as well as carefully considering the mechanics of milling, a theoretical force model for helical end milling can be developed.

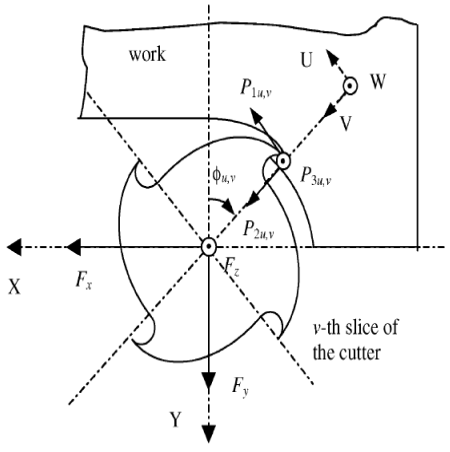


**Fig. 4. Coordinate systems for the *v*th slice of the milling cutter.**

The total forces acting on the cutter are the sum of the forces on each tooth segment. With $P_{1u,v}$, $P_{2u,v}$ and $P_{3u,v}$ calculated, the cutting force on this edge segment can be expressed in terms of the fixed coordinate system X Y Z. Thus the total cutting forces of the helical end milling cutter at the present instance, $F_x$, $F_y$ and $F_z$, as shown in Fig. 4, can be determined by the following equations,

$$F_x(t) = \sum_{v=1}^{r}\sum_{u=1}^{Nt}(P_{1u,v}\cos\phi_{u,v} + P_{2u,v}\sin\phi_{u,v}) \quad (8)$$

$$F_y(t) = \sum_{v=1}^{r}\sum_{u=1}^{Nt}(-P_{1u,v}\sin\phi_{u,v} + P_{2u,v}\cos\phi_{u,v}) \quad (9)$$

$$F_z(t) = \sum_{v=1}^{r} \sum_{u=1}^{Nt} P_{3u,v} \qquad (10)$$

A windows-based simulation system has been developed based on this model, which predictsthe milling forces from input data of work piece material properties, tool geometry and cutting conditions.

### 3.4 Modelling with MathCAD 8 Professional

The MathCAD program is developed for finding the variation of cutting forces with respect to cutting parameters. The sample MathCAD 8 professional Window is shown in Fig. 5 and the results obtained from the MathCAD simulation has been tabulated in Table. 2 as below.

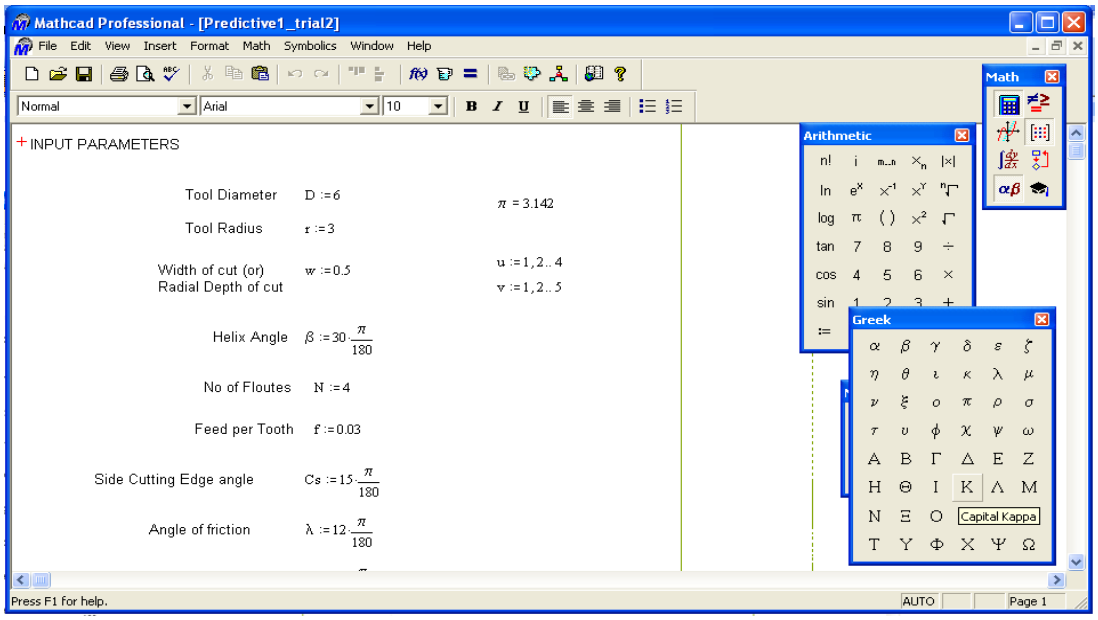


**Fig. 5.MathCAD 8 Professional Window**

## IV. EXPERIMENTAL VERIFICATION AND COMPARISON OF CUTTING FORCE COMPONENTS

Experiments were carried out on a 3-axis Vertical CNC milling machine fitted with 5 kW high-speed spindle, which has a maximum speed of 40,000 rpm. The workpiece used was aluminum alloy of 6210 grade. A two-flute Titanium Nitride coated solid carbide endmill was used for machining. The diameter of the endmill, helix angle, and radial rake angle are 6 mm, 30°and 2° respectively. The schematic diagram of the experimental set-up is shown in Fig. 6. A Kistlerpiezo-electric 3– component dynamometer was used for measuring the forces. Teknonix make oscilloscope was used for recording these forces in terms of voltage.

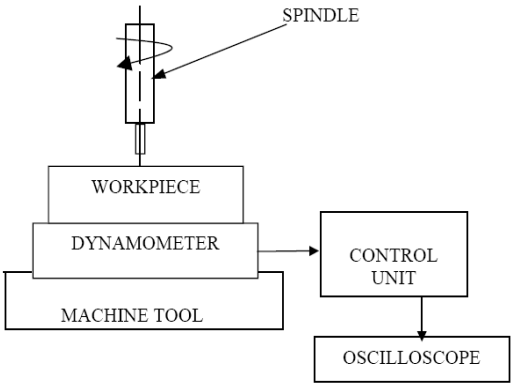


**Fig. 6. Schematic representation of experimental set-up**

The material properties of work piece such as young's modulus, poisson's ratio and density are considered as 61500 N/mm$^2$, 0.33 and 2700*10$^{-9}$kg/mm$^3$. The forces correspond to a cutting velocity of 453 m/min (spindle

speed of 24000 rpm using a 6 mm cutter) and for feed rates varying from 1000 mm/min to 2500 mm/min are shown in Table 1.

**Table 1. Experimental Cutting and feed forces**

| S.No | Feed (mm/min) | Fx (N) | Fy (N) |
|---|---|---|---|
| 1. | 1000 | 16 | 12 |
| 2. | 1500 | 21 | 16 |
| 3. | 2000 | 26 | 21 |
| 4. | 2500 | 30 | 26 |

**Table 2. Variation of cutting forces and chip thickness with input Parameters taken from MathCAD Simulation**

| Sl.No | Parameter | | Fx (N) | Fy (N) | Fz (N) | $t_1$ (mm) |
|---|---|---|---|---|---|---|
| 1. | Feed per tooth (mm) | 0.03 | -13.74 | 10.83 | 0.86 | 0.017 |
| | | 0.035 | -16.03 | 12.63 | 1.01 | 0.02 |
| | | 0.04 | -18.32 | 14.44 | 1.15 | 0.023 |
| | | 0.045 | -20.61 | 16.24 | 1.3 | 0.026 |
| | | 0.05 | -22.9 | 18.04 | 1.44 | 0.029 |
| 2. | Width of cut (mm) | 0.3 | -7.63 | 6.02 | 0.05 | 0.014 |
| | | 0.4 | -10.57 | 8.33 | 0.67 | 0.016 |
| | | 0.5 | -13.74 | 10.83 | 0.86 | 0.017 |
| | | 0.6 | -17.17 | 13.53 | 1.09 | 0.019 |
| | | 0.7 | -20.9 | 16.48 | 1.32 | 0.02 |
| 3. | Axial Depth of cut (mm) | 3 | 16.25 | 7.55 | 0.864 | 0.017 |
| | | 4 | -2.60E-13 | 7.30E-14 | 0.864 | 0.017 |
| | | 5 | -13.74 | 10.827 | 0.864 | 0.017 |
| | | 6 | -18.41 | 23.425 | 0.864 | 0.017 |
| | | 7 | -18.79 | 32.91 | 0.864 | 0.017 |
| 4. | Time (micro sec) | 175 | 10.827 | 13.737 | 0.867 | 0.017 |
| | | 180 | 17.477 | -0.685 | 0.867 | 0.017 |
| | | 185 | 9.719 | -14.542 | 0.867 | 0.017 |
| | | 190 | -6.052 | -16.41 | 0.867 | 0.017 |
| | | 195 | -16.833 | -4.749 | 0.867 | 0.017 |
| | | 200 | -13.737 | 10.827 | 0.867 | 0.017 |
| | | 205 | 0.685 | 17.477 | 0.867 | 0.017 |
| | | 210 | 14.542 | 9.719 | 0.867 | 0.017 |
| | | 215 | 16.41 | -6.052 | 0.867 | 0.017 |
| | | 220 | 4.749 | -16.833 | 0.867 | 0.017 |
| | | 225 | -10.827 | -13.737 | 0.867 | 0.017 |
| | | 230 | -17.477 | 0.685 | 0.867 | 0.017 |
| | | 235 | -9.719 | 14.542 | 0.867 | 0.017 |
| | | 240 | 6.052 | 16.41 | 0.867 | 0.017 |
| | | 245 | 16.833 | 4.749 | 0.867 | 0.017 |

The comparison between the experimental and simulation results shows a good agreement for particular selected inputs. The value Fz is omitted in the experiments as it has very less values when compared with cutting (Fx) and feed (Fy) forces. The results from the MathCAD simulation are plotted as graphs for inference.

### 4.1 Effect of feed on force and chip thickness

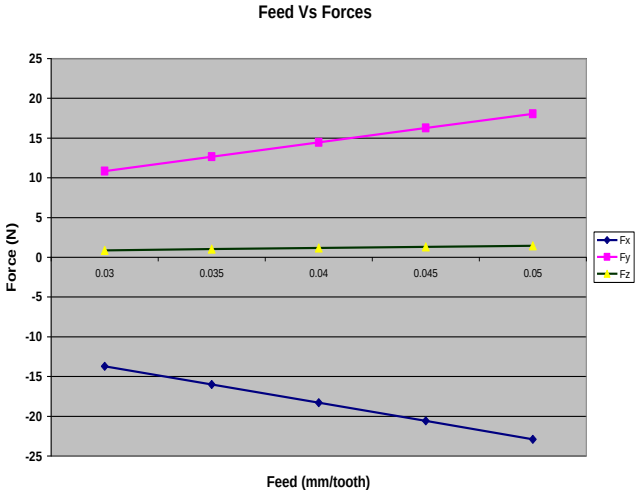


**Fig. 7. Effect of feed on cutting forces**

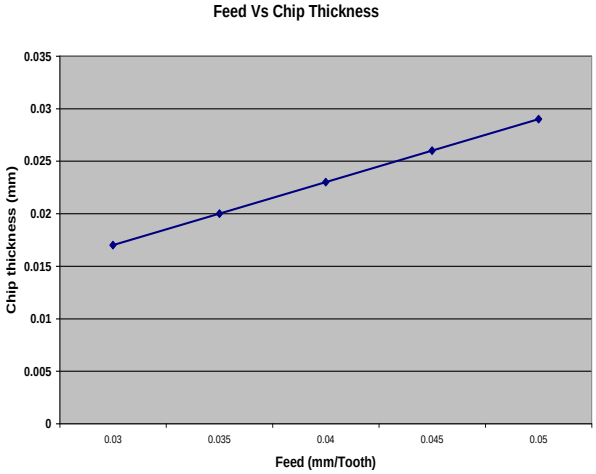


**Fig. 8. Effect of feed on chip thickness**

The cutting force component Fz has very less impact by change in feed (Fig. 7.) and other force components and chip thickness (Fig. 8.) varies with feed.

### 4.2 Effect of width of cut on force and chip thickness


**Fig. 9. Effect of width of cut on cutting forces**

The cutting force component Fz has very less impact by change in cut width (Fig. 9.) and other force components and chip thickness (Fig. 10.) varies with width of cut.

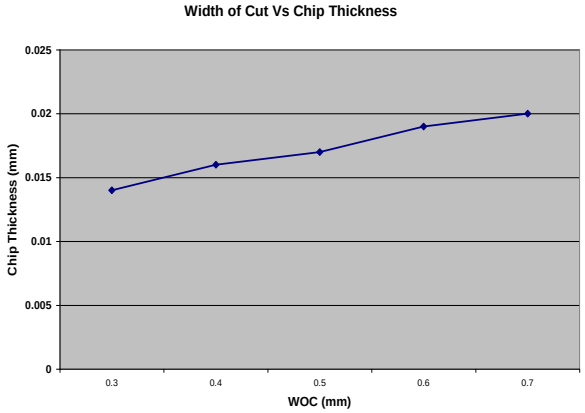


**Fig. 10. Effect of width of cut on chip thickness**

### 4.3 Effect of axial depth of cut on force and chip thickness

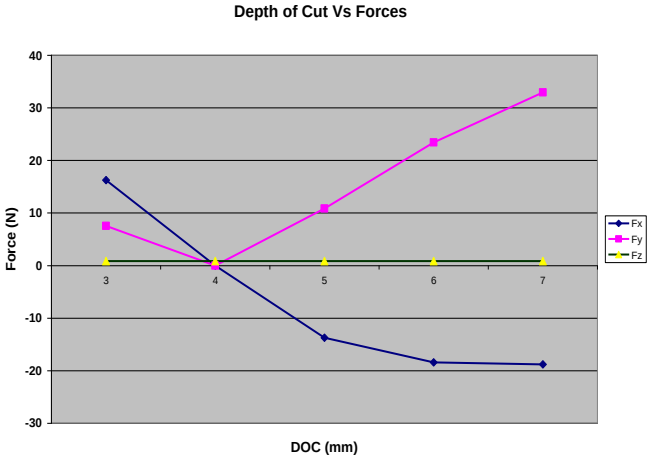


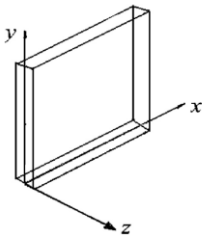


**Fig. 11. Effect of axial depth of cut on cutting forces**

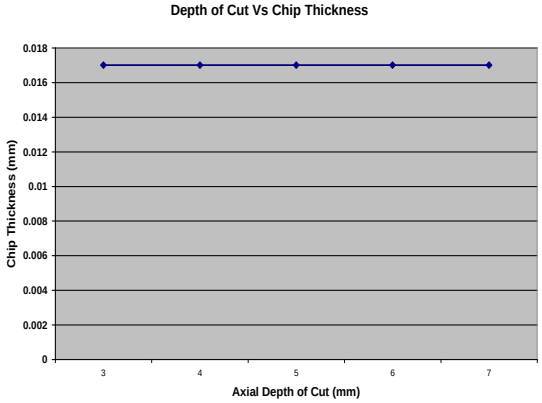


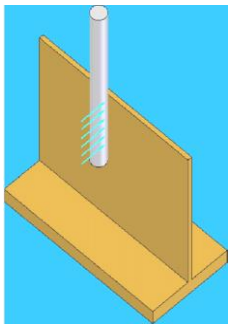

**Fig. 12. Effect of axial depth of cut on chip thickness**

The force Fz has no impact by axial depth of cut (Fig. 11) and chip thickness **(Fig. 12) is independent of axial depth of cut.**

### 4.4 Simulation of forces with tool engagement time

When the machining process is conducted the cutting for vary only at the engagement time of tool. Hence it is the cyclic process which repeats itself. The force components Fx and Fy is simulated as graph (Fig. 13) with respect to engagement time (t).

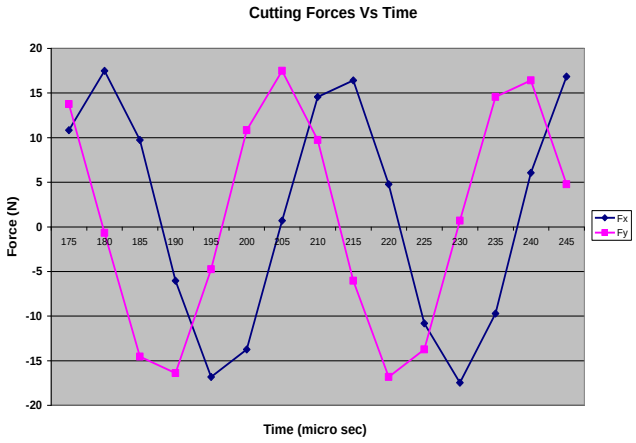


**Fig. 13. Cutting force simulation with engagement time**

## V. DEFORMATION ANALYSIS OF THIN-RIBS

### 5.1Assumptions

1) The displacement of every point on the plates does not change along the thickness, which is equal to the deformations of the plate middle plane.
2) Straight normal line hypothesis: the normal line is still straight and vertical to the middle plane both pre-deformations and after deformations.
3) The normal stress applied on the plane that is parallel to the middle plane is very small. It thus can be ignored.

The size of the thin-walled plate used in this paper is 100mm×40mm×2mm. The material of the part is aluminum alloy with Young's modulus of 61500N/mm$^2$, Poisson's ratio of 0.33, the axial depth of cut is 10mm and density is 2700 x $10^{-9}$ Kg/mm$^3$.

## VI. ERROR COMPENSATION PROFILE

The error compensation profile is drawn and is to be verified analytically and experimentally. The part deflection at the machining plane P shown in Fig. 14. When machining at point j the profile is created for compensation.

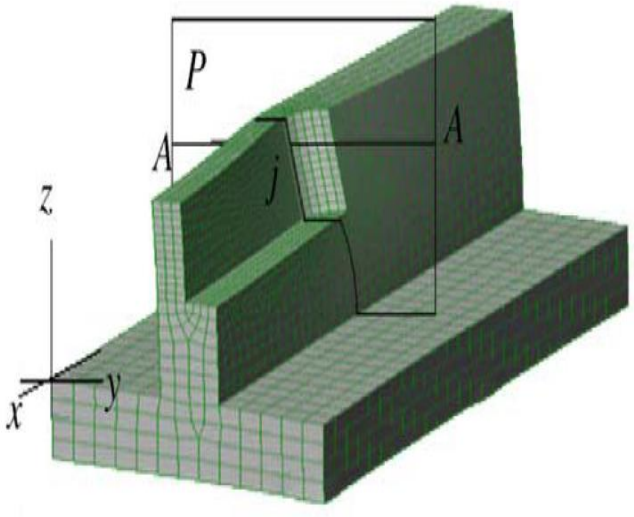


**Fig. 143-D views of section A–A at position *j* in plane-P.**

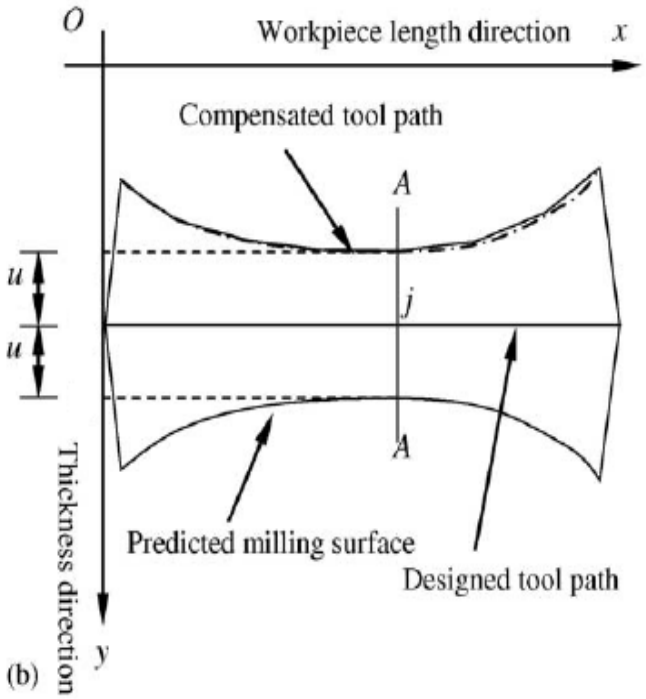


**Fig. 15 2-D view of Error compensation profilein section A–A at cutting position *j*.**

The 2-D view with section A-A (Fig. 15) shows the profile is created at the top end of the work piece with thickness. The gradual reduction in machining depth will reduce profile curve into straight line since bottom of the work piece will not have surface error. U is half thickness of the work piece, i.e., the parameter to measure surface error at each plane.

## VII. DISCUSSION

The static analysis is carried out using FEA software ANSYS. The influences of unit linear load, cutter location and part thickness on deformation of thin-walled parts are analysed. The deformation values for the influence of unit linear load, cutter location and part thickness were found. The following are the discussions made with the depicted graphs.

- The part deformations are gradually increased from bottom to top.
- The deformations distribution is symmetric with respect to the middle line ($x$ = 50 mm).
- The part deformations reach the maximum value at the location of $x$=0 and 100mm, while the minimum deformations are at the location of $x$ = 50mm.
- The maximal deformations are in inverse proportion to the wall thickness when the same unit linear load is applied.

## VIII. CONCLUSIONS

The paper reports on error compensation approach that takes into account the deflection of thin-wall parts during machining. The modified CNC programs can optimize the tool path to partially compensate the surface profile errors caused by deflection.

The error prediction and compensation methodology can be integrated with main stream NC part program simulation and verification packages such as VERICUT.

The reported single level error compensation strategy is a part of an on-going research. It is expected that the error will be further reduced by introducing a multi-level optimization method, the results of which will be reported in due course.

## REFERENCES


[1]. He Ning, Wang Zhigang, Jiang Chengyu, Zhang Bing, "Finite element method analysis and control stratagem for machining deformation of thin-walled components", Journal of Materials Processing Technology 139 (2003) 332–336

[2]. Jitender K. Rai, Paul Xirouchakis, "Finite element method based machining simulation environment for analyzing part errors induced during milling of thin-walled components", International Journal of Machine Tools & Manufacture 48 (2008) 629–643

[3]. Liu Gang, " Study on deformation of titanium thin-walled part in milling process", journal of materials processing technology 209 (2009) 2788–2793

[4]. Tang Aijun, Liu Zhanqiang, "Deformations of thin-walled plate due to static end milling force", journal of materials processing technology 206 (2008) 345–351

[5]. S. Ratchev, S. Liu , W. Huang, A.A. Becker, "Milling error prediction and compensation in machining of low-rigidity parts", International Journal of Machine Tools & Manufacture 44 (2004) 1629–1641

[6]. Tang Aijun, Liu Zhanqiang, Ma Hailong, "Modeling and Simulation of Big Deformations of Thin walled Plate in End Milling Process", Proceedings of the IEEE International Conference on Automation and Logistics August 18 - 21, 2007, Jinan, China

[7]. S. Ratchev, S. Liu , A.A. Becker, "Error compensation strategy in milling flexible thin-wall parts", Journal of Materials Processing Technology 162–163 (2005) 673–681

[8]. H.Z. Li, W.B. Zhang, X.P. Li, "Modelling of cutting forces in helical end milling using a predictive machining theory", International Journal of Mechanical Sciences 43 (2001) 1711–1730

[9]. S. Ratchev, S. Liu, W. Huang, A.A. Becker, "A flexible force model for end milling of low-rigidity parts", Journal of Materials Processing Technology 153–154 (2004) 134–138

[10]. WeifangChen a, JianbinXue a, DunbingTang a, HuaChen a, ShaopengQub, "Deformation prediction and error compensation in multilayer milling processes for thin-walled parts", International Journal of Machine Tools & Manufacture 49 (2009) 859–864

[11]. F. Cusa, U. Zuperla, V. Gecevska, "High-speed milling of light metals", journal of Achievements in Materials and Manufacturing Engineering, VOLUME 24 ISSUE 1 September 2007

[12]. S. Zhang & J. F. Li & J. Sun & F. Jiang, "Tool wear and cutting forces variation in high-speed end-milling Ti-6Al-4V alloy", Received: 1 February 2009 / Accepted: 23 April 2009, Springer-Verlag London Limited 2009

[13]. E. Budak, "Analytical models for high performance milling. Part I: Cutting forces, structural deformations and tolerance integrity", International Journal of Machine Tools & Manufacture 46 (2006) 1478–1488

[14]. Hassan El-Hofy, " Fundamentals of machining processes", Taylor & Francis, 2007, pp 21-27

[15]. P.H.Joshi, " Machine Tool Design Hand Book", TMH 2007, pp 665-674.